Available online at www.sciencedirect.com
SCIENCE DIRECT®
Chemical Physics Letters 376 (2003) 103–107
CHEMICAL PHYSICS LETTERS
www.elsevier.com/locate/cplett

Raman scattering study of rutile SnO_2 nanobelts synthesized by thermal evaporation of Sn powders

S.H. Sun [a], G.W. Meng [a,b,*], G.X. Zhang [c], T. Gao [a], B.Y. Geng [a], L.D. Zhang [a], J. Zuo [d]

[a] Institute of Solid State Physics, Chinese Academy of Sciences, P.O. Box 1129, Hefei 230031, PR China
[b] Department of Materials Science and Engineering, Rensselaer Polytechnic Institute, Troy, NY 12180, USA
[c] Anhui Institute of Optics and Fine Mechanics, Chinese Academy of Sciences, Hefei 230031, PR China
[d] Structure Research Laboratory, University of Science and Technology of China, Chinese Academy of Sciences, Hefei 230026, PR China

Received 6 April 2003; in final form 6 June 2003
Published online: 28 June 2003

Abstract

The Raman spectrum of single-crystalline rutile tin dioxide (SnO_2) nanobelts synthesized by thermal evaporation of tin powders was studied. Three Raman shifts (474, 632, 774 cm^{-1}) showed the typical feature of the rutile phase of the as-synthesized SnO_2 nanobelts. It was found that two infrared (IR)-active modes (313 and 690 cm^{-1}) appeared in Raman spectrum and some peaks were broadened.

1. Introduction

Tin dioxide (SnO_2), a very important n-type semiconductor with a wide band gap ($E_g = 3.6$ eV, at 300 K), is well known for its potential applications in gas sensors [1], transparent conducting electrodes [2], transistors [3], and solar cells [4]. So far, considerable effort has been devoted to the synthesis of nanostructured SnO_2 materials, including nanoparticles [1], nanowires [5], and nanorods [6].

Recently, nanobelts, a new family in the realm of 1D nanomaterials, are regarded as an ideal system to fully understand dimensionally confined transport phenomena, and may act as valuable units to construct nanodevices owing to their well-defined geometry [7]. A series of binary semiconducting oxide nanobelts (or nanoribbons) [7–9], nitride nanobelts [10,11], and pure metal Zn nanobelts [12], have been prepared. Among them, SnO_2 nanobelts have been successfully synthesized by thermal evaporation of different source materials, such as oxide (SnO_2 or SnO) powders [7,13], mixture of Sn foil and SnO powders [14], metal Sn and $Fe(NO_3)_3$ mixture [15], under controlled conditions. Previously, we synthesized large quantities of SnO_2 nanobelts at 800 °C by using Sn powders

* Corresponding author. Fax: +86-551-5591434.
E-mail addresses: shsuncn@hotmail.com (S.H. Sun), gwmeng@issp.ac.cn, mengg2@rpi.edu (G.W. Meng).

0009-2614/03/$ - see front matter © 2003 Elsevier Science B.V. All rights reserved.
doi:10.1016/S0009-2614(03)00965-5

as source material under normal atmospheric pressure, without using any other additional oxidants or catalysts [16].

As is well known, Raman scattering is a useful tool for the characterization of nanosized materials and a qualitative probe of the presence of lattice defects in solids, e.g., the crystalline quality can be judged from the peak shapes and the selection rules. However, until now, Raman scattering properties of SnO_2 nanobelts have been little explored. In this Letter, three fundamental Raman scattering peaks, which are in good agreement with those of a rutile SnO_2 single crystal [17], were attained, and two infrared (IR)-active modes ($E_u(3)$ TO and A_{2u}LO) were also found at Raman spectrum. The three fundamental Raman peaks were broadened compared with those of rutile bulk SnO_2.

2. Experimental

SnO_2 nanobelts were synthesized by thermal evaporation of tin powders under controlled conditions without catalysts. A detailed experimental procedure for the preparation of SnO_2 nanobelts was described elsewhere [16]. Briefly, pure Sn powders were placed in an alumina boat, which was put in the middle of the quartz tube inserted in a horizontal tube furnace. The reaction chamber was heated to 800 °C rapidly from room temperature under flowing Ar (100 sccm) atmosphere. Subsequently, the furnace was kept at 800 °C for 2 h, and SnO_2 nanobelts was obtained via a vapor–solid (VS) process.

The as-synthesized products were characterized by X-ray powder diffraction (XRD) (Philips PW 1710 with Cu-K_α radiation), scanning electron microscopy (SEM, JEOL JSM 6700F), high-resolution transmission electron microscopy (HRTEM, JEOL 2010, operated at 200 kV). The Raman spectra were obtained using a LABRAM-HR Confocal Laser MicroRaman spectrometer at room temperature. A green line (514.5 nm) of Ar^+ laser was used as the excitation source. The electron paramagnetic resonance (EPR) spectrum was obtained by using a Bruker ER-200D electron paramagnetic resonance device with 10 dB (20 mW).

3. Results and discussion

XRD patterns (Fig. 1a) from the as-synthesized products show that the sample is tetragonal rutile structure SnO_2 with lattice constants of $a = 4.734$ Å and $c = 3.185$ Å, being consistent with the standard values of bulk SnO_2 (JCPDS 21-1250). A representative SEM image (Fig. 1b) of several

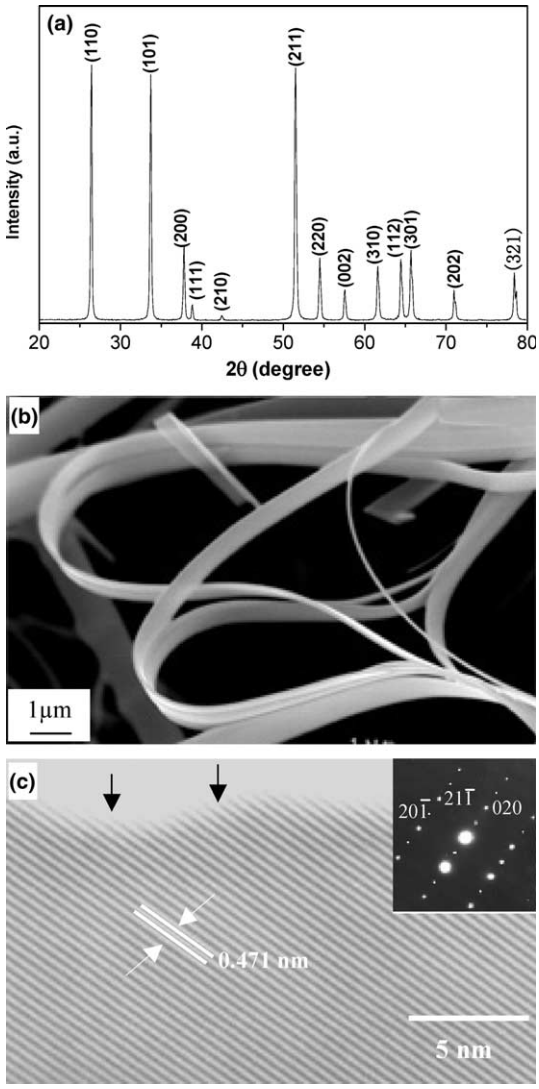

Fig. 1. (a) The XRD pattern recorded from the as-synthesized SnO_2 nanobelts. (b) A typical SEM image of the as-synthesized product. (c) HRTEM image of SnO_2 nanobelts, inset showing the corresponding SAED pattern.

curved SnO_2 1D nanostructures reveals that their geometrical shape is beltlike, which is distinct from those of nanowires and nanotubes. Their typical widths and thickness are in the range of 60–250 nm and 10–30 nm, respectively. An HRTEM image recorded near the side-edge of the SnO_2 nanobelt along the direction perpendicular to the wide surface of the nanobelt is given in Fig. 1c. It shows that the surface of the nanobelt is clean and abrupt on an atomic scale with some atom-high steps and point defects, as shown by the black arrowheads, and there is no amorphous layer covering on the surface. The electron diffraction pattern (inset in Fig. 1c) indicates that the SnO_2 nanobelt grows along the [1 0 1] direction. All results confirm the formation of rutile SnO_2 nanobelts.

Rutile SnO_2 belongs to the space group D_{4h}^{14}, of which the normal lattice vibration at the Γ point of the Brillouin zone is given on the basis of group theory [18]

$$\Gamma = 1A_{1g} + 1A_{2g} + 1A_{2u} + 1B_{1g} + 1B_{2g} + 2B_{1u} + 1E_g + 3E_u.$$

Among them, the active Raman modes are B_{1g}, E_g, A_{1g}, and B_{2g}, and consequently four first-order Raman spectra are observed.

Fig. 2 shows the room temperature Raman scattering spectra of the as-synthesized SnO_2 nanobelts (a) and that of bulk SnO_2 (b). Three fundamental Raman peaks at 474, 632, and 774 cm^{-1}, corresponding to the E_g, A_{1g}, and B_{2g} vibration modes, respectively, are observed, in good agreement with those for the rutile bulk SnO_2 (Fig. 2b). Thus, these peaks further confirm that the as-synthesized SnO_2 nanobelts possess the characteristics of the tetragonal rutile structure [5]. In addition to the fundamental Raman peaks of rutile SnO_2, the other two weak Raman peaks at about 313 and 690 cm^{-1} are also observed, whereas these two Raman peaks are not detected in the rutile bulk SnO_2 (Fig. 2b). According to [19], these two weak Raman bands at 314 and 690 cm^{-1} seem to correspond to IR-active $E_u(3)$ TO and A_{2u}LO (TO is the mode of the transverse optical phonons, LO is the mode of the longitudinal optical phonons) modes, respectively. This situation is similar to the one recently reported by Liu et al. [6] for rutile SnO_2 nanorods. From Fig. 2, it also can be seen that the three fundamental peaks of SnO_2 nanobelts are broadened as compared with those of rutile bulk SnO_2 (in Fig. 2b). The full width at half maximum (FWHM) of E_g, A_{1g}, and B_{2g} modes of SnO_2 nanobelts are 14.5, 9.3, and 13.8 cm^{-1}, respectively, while the FWHMs of the corresponding modes of bulk SnO_2 are 4.0, 8.8, and 11.6 cm^{-1}, respectively. It is obvious that E_g mode is broadened most, followed by B_{2g} mode, and A_{1g} mode is broadened a little. The reasons are analyzed as following.

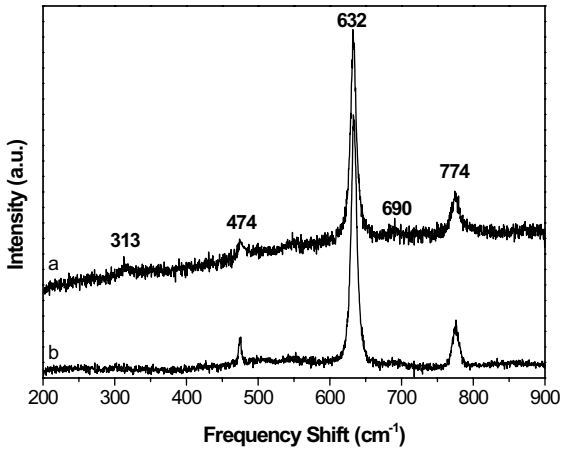

Fig. 2. (a and b) Room-temperature Raman spectra of an individual SnO_2 nanobelt and the bulk SnO_2, respectively.

Abello and his co-workers [19] proposed that the relaxation of the $k = 0$ selection rule is progressive when the rate of disorder increases or the size decreases, and infrared (IR) modes can become weakly active when the structural changes induced by disorder and size effects take place. And also, it is well known that in an infinite perfect crystal only the phonons near the center of the Brillouin zone (BZ) contribute to the scattering of incident radiation due to the momentum conservation rule between phonons and incident light. As the crystallite is reduced to nanoscale, the phonon scattering will not be limited to the center of the Brillouin zone, and phonon dispersion near the center of Brillouin zone must also be considered. As a result, the symmetry-forbidden modes will be observed, in addition to the shift and broadening of the first-order optical phonon. Campbell and

Fauchet [20] and Richter et al. [21] believed that while microcrystals are smaller than 300 Å, it would lead to down shift and broadening of the Raman spectrum of silicon. Chuu et al. [22] believed that for small CdS crystallites with diameters ranging from 30 to 1000 Å the size effect is manifested by addition to the normal modes of the single crystal. Here, one dimension of the as-synthesized SnO_2 nanobelts is small enough (10–30 nm in width). So, it seems reasonable to believe that the broadening of the peaks in Raman spectrum of SnO_2 nanobelts is induced by the size effect of the small thickness (10–30 nm) of SnO_2 nanobelts. But it is worth noting that the E_g mode (at 474 cm^{-1}) is much more broadened, compared with A_{1g} (at 632 cm^{-1}) and B_{2g} (at 774 cm^{-1}) modes.

In addition to the nanosize effect, another influence on E_g mode can be attributed to the existence of oxygen vacancies [15,23]. As the E_g mode is the result of two oxygen atoms vibrating parallel to the *c* axis, but in opposite direction, it is more sensitive to oxygen vacancies than other modes [24]. The electron paramagnetic resonance (EPR) results (in Fig. 3, $g = 2.0069$) reveal that there are many single ionized oxygen vacancies (Vo^{+}) in our SnO_2 nanobelts because other oxygen vacancies (Vo or Vo^{++}) are not paramagnetic [25]. So, the E_g mode is broadened most, the other two modes influenced a little. Therefore, we propose that single ionized oxygen vacancies (Vo^{+}) be most probably responsible for the broadening of the E_g mode of SnO_2 nanobelts besides the nanosize effect.

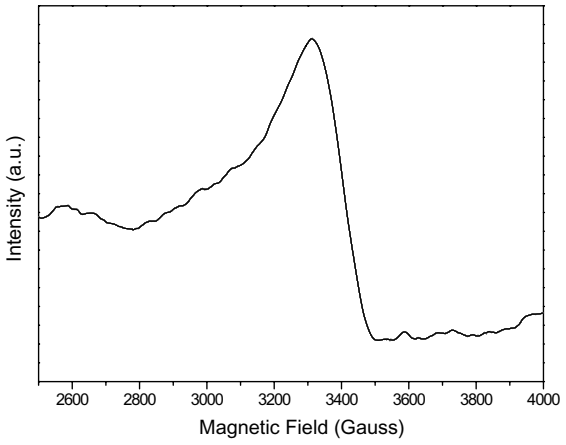

Fig. 3. X-band (9.45 GHz) EPR traces for the SnO_2 nanobelts at room temperature.

It should be noted that there were no additional oxidants or catalysts used in the process, and the XRD results proved that the products are pure rutile SnO_2. Thus, the possibility for the changes of the Raman spectrum originating from the impurity contaminants seems extremely unlikely in the present study. And also, since the energy of incident light (2.41 eV) used in our experiment is smaller than that of band gap ($E_g = 3.6$ eV) of SnO_2, the 'Fano resonance' would not happen in our experiment. Based on the earlier studies, we believe that the appearance of the two new modes and the broadening of the peaks can attribute to the relaxation of momentum conservation selection rule, when the rate of disorder increases or the size decreases. The oxygen vacancy influenced E_g mode most. Further work is under way.

4. Conclusions

In summary, a systematic Raman study of SnO_2 nanobelts synthesized by thermal evaporation method has been reported. Three fundamental Raman modes of rutile SnO_2 nanobelts were observed. We tend to think the broadening of three fundamental peaks and the IR-active $E_u(3)$ TO and A_{2u} LO of SnO_2 nanobelts becoming Raman-active can attribute to the nanoscale morphology of the nanobelts. In addition, the broadening of the E_g mode can be mainly due to oxygen vacancies besides nanosize effect.

Acknowledgements

We are grateful for financial support of the Ministry of Sciences and Technology of China (Grant No. G1999064501) and the Natural Science Foundation of China (Grant No. 19974055). G.W. Meng is grateful to RPI and Philip Morris USA for financial support. Profs. Y.Q. Mao, Y. Qin, S.Y. Zhang, and L. Chen are also thanked for providing the research facility.

References

[1] E.R. Leite, I.T. Weber, E. Longo, J.A. Varela, Adv. Mater. 12 (2000) 966.
[2] Y.S. He, J.C. Campbell, R.C. Murphy, M.F. Arendt, J.S. Swinnea, J. Mater. Res. 8 (1993) 3131.
[3] G. Sberveglieri, Sensory Actuators B 6 (1992) 64.
[4] S. Ferrere, A. Zaban, B.A. Gsegg, J. Phys. Chem. B 101 (1997) 4490.
[5] W.Z. Wang, C.K. Xu, G.H. Wang, Y.K. Liu, C.L. Zheng, J. Appl. Phys. 92 (2002) 2740.
[6] Y.K. Liu, C.L. Zheng, W.Z. Wang, C.R. Yin, G.H. Wang, Adv. Mater. 13 (2001) 1883.
[7] Z.W. Pan, Z.R. Dai, Z.L. Wang, Science 291 (2001) 1947.
[8] Z.W. Pan, Z.R. Dai, Z.L. Wang, Appl. Phys. Lett. 80 (2002) 309.
[9] J. Zhang, L. Zhang, X. Peng, X. Wang, Appl. Phys. A 73 (2001) 733.
[10] Y.H. Gao, Y. Bando, T. Sato, Appl. Phys. Lett. 79 (2001) 4565.
[11] S.Y. Bae, H.W. Seo, J. Park, H. Yang, J.C. Park, S.Y. Lee, Appl. Phys. Lett. 81 (2002) 126.
[12] Y.W. Wang, L.D. Zhang, G.W. Meng, C.H. Liang, G.Z. Wang, S.H. Sun, Chem. Commun. 24 (2001) 2632.
[13] Z.R. Dai, Z.W. Pan, Z.L. Wang, Solid State Commun. 118 (2001) 351.
[14] Z.R. Dai, J.L. Gole, J.D. Stout, Z.L. Wang, J. Phys. Chem. B 106 (2002) 1274.
[15] J.Q. Hu, X.L. Ma, N.G. Shang, Z.Y. Xie, N.B. Wong, C.S. Lee, S.T. Lee, J. Phys. Chem. B 106 (2002) 3823.
[16] S.H. Sun, G.W. Meng, Y.W. Wang, T. Gao, M.G. Zhang, Y.T. Tian, X.S. Peng, L.D. Zhang, Appl. Phys. A 76 (2003) 287.
[17] J.F. Scott, J. Chem. Phys. 33 (1970) 852.
[18] S.P.S. Porto, P.A. Fleury, T.C. Damen, Phys. Rev. 154 (1967) 522.
[19] L. Abello, B. Bochu, A. Gaskov, S. Koudryavtseva, G. Lucazeau, M. Roumyantesva, J. Solid State Chem. 135 (1998) 78.
[20] I.H. Campbell, P.M. Fauchet, Solid State Commun. 58 (1986) 739.
[21] H. Richter, P.M. Wang, L. Ley, Solid State Commun. 39 (1981) 625.
[22] D.S. Chuu, C.M. Dai, W.F. Hsieh, C.T. Tsai, J. Appl. Phys. 69 (1991) 8402.
[23] J.C. Paker, R.W. Siegel, Appl. Phys. Lett. 57 (1990) 943.
[24] J.K. Jian, X.L. Chen, T. Xu, Y.P. Xu, L. Dai, M. He, Appl. Phys. A 75 (2002) 695.
[25] M.J. Zheng, L.D. Zhang, G.H. Li, X.Y. Zhang, X.F. Wang, Appl. Phys. Lett. 79 (2001) 839.